
ASYNCHRONOUS STOCHASTIC GRADIENT DESCENT WITH DECOUPLED BACKPROPAGATION AND LAYER-WISE UPDATES

**Cabrel Teguemne Fokam¹, Khaleelulla Khan Nazeer²,
Lukas König¹, David Kappel¹, Anand Subramoney³**

¹Institut für Neuroinformatik, Ruhr Universität Bochum, Germany

²Chair of Highly-Parallel VLSI Systems and Neuro-Microelectronics, Technische Universität Dresden, Germany

³Department of Computer Science, Royal Holloway, University of London, United Kingdom

{cabrel.teguemnefokam, lukas.koenig, david.kappel}@ini.rub.de

khaleelulla.khan.nazeer@tu-dresden.de

anand.subramoney@rhul.ac.uk

ABSTRACT

The increasing size of deep learning models has created the need for more efficient alternatives to the standard error backpropagation algorithm, that make better use of asynchronous, parallel and distributed computing. One major shortcoming of backpropagation is the interlocking between the forward phase of the algorithm, which computes a global loss, and the backward phase where the loss is backpropagated through all layers to compute the gradients, which are used to update the network parameters. To address this problem, we propose a method that parallelises SGD updates across the layers of a model by asynchronously updating them from multiple threads. Furthermore, since we observe that the forward pass is often much faster than the backward pass, we use separate threads for the forward and backward pass calculations, which allows us to use a higher ratio of forward to backward threads than the usual 1:1 ratio, reducing the overall staleness of the parameters. Thus, our approach performs asynchronous stochastic gradient descent using separate threads for the loss (forward) and gradient (backward) computations and performs layer-wise partial updates to parameters in a distributed way. We show that this approach yields close to state-of-the-art results while running up to $2.97\times$ faster than Hogwild! scaled on multiple devices (Locally-Partitioned-Asynchronous-Parallel SGD). We theoretically prove the convergence of the algorithm using a novel theoretical framework based on stochastic differential equations and the drift diffusion process, by modeling the asynchronous parameter updates as a stochastic process.

1 INTRODUCTION

Scaling up modern deep learning models requires massive resources and training time. Asynchronous parallel and distributed methods for training them using backpropagation play a very important role in easing the demanding resource requirements for training these models. Backpropagation (BP) (Werbos, 1982) has established itself as the de facto standard method for learning in deep neural networks (DNN). Although BP achieves state-of-the-art accuracy on literally all relevant machine learning tasks, it comes with a number of inconvenient properties that prohibit an efficient implementation at scale.

BP is a two-phase synchronous learning strategy in which the first phase (forward pass) computes the training loss, \mathcal{L} , given the current network parameters and a batch of data. In the second phase, the gradients are propagated backwards through the network to determine each parameter's contribution to the error, using the same weights (transposed) as in the forward pass (see Equation 1). BP suffers from update locking, where a layer can only be updated after the previous layer has been updated. Furthermore, the computation of gradients can only be started after the loss has been calculated in the forward pass.

Moreover, the backward pass usually requires approximately twice as long as the forward pass (Kumar et al., 2021). The bulk of the computational load comes from the number of matrix multiplications required during each phase. If we consider a DNN with M layers, then at any layer $m \leq M$ with pre-activations $z_m = \theta_m \mathbf{y}_{m-1}$ and post-activations $\mathbf{y}_m = f(z_m)$, the computations during the forward pass are dominated by one matrix multiplication $\theta_m \mathbf{y}_{m-1}$. During the backward pass, the computations at layer m are dominated by two matrix multiplications:

$$\frac{\partial \mathcal{L}}{\partial \theta_m} = f'(\theta_m \mathbf{y}_{m-1}) \times \mathbf{y}_{m-1}^\top \quad \text{and} \quad \frac{\partial \mathcal{L}}{\partial \mathbf{y}_{m-1}} = f'(\theta_m \mathbf{y}_{m-1}) \times \theta_m^\top, \quad (1)$$

approximately doubling the compute budget required for the backward pass compared to the forward pass. In Eq. 1, θ_m denotes the network weights at layer m and f' the partial derivative with respect to θ_m . This imbalance between forward and backward phase further complicates an efficient parallelization of BP, particularly in heterogeneous settings.

In this work, we propose a new approach to parallelize training of deep networks on non-convex objective functions by asynchronously performing the forward and backward passes at a layer-wise granularity in multiple separate threads that make lock-free updates to the parameters in shared memory. The lock-free updates address the locking problem, performing layer-wise updates mitigates the issue of conflicts between parameter updates, and performing the backward pass and updates using more threads than the forward pass mitigates the staleness problem. Specifically, the imbalance in execution time between forward and backward passes is taken care of by having twice as many backward threads than forward threads, breaking the 1:1 ratio of vanilla Backpropagation, therefore significantly speeding-up the training process.

In summary, the contributions of this paper are as follows:

1. We introduce a novel asynchronous formulation of Backpropagation which allows the forward pass and the backward pass to be executed separately and in parallel, which allows us to run more backward than forward threads. This approach accounts for the unequal time required by the forward and backward passes.
2. We propose to asynchronously update the model’s parameters at a layer-wise granularity without using a locking mechanism which reduces staleness.
3. We give convergence guarantees of the algorithm to a stationary distribution centered around the local optima of conventional BP.
4. We show that the algorithm can reach state-of-the-art performances while being significantly faster than competing asynchronous algorithms.

2 RELATED WORK

Asynchronous stochastic gradient descent (SGD). Asynchronous SGD has a long history, starting from Baudet (1978); Bertsekas & Tsitsiklis (2015). Hogwild! (Recht et al., 2011) allows multiple processes to perform SGD without any locking mechanism. Kungurtsev et al. (2021) proposed to partition the models parameters across the workers on the same device to perform SGD on the partitions. Chatterjee et al. (2022) decentralizes Hogwild! and PASSM+ to allow parameters or their partitions to be located on multiple devices and perform Local SGD on them. Zheng et al. (2017) compensated the delayed gradients with a gradient approximation at the current parameters. Unlike these methods, we don’t run multiple forward passes in parallel and don’t need any gradient compensation scheme.

Nadiradze et al. (2021) provides a theoretical framework to derive convergence guarantees for a wide variety of distributed methods. Mishchenko et al. (2022) proposes a method of “virtual iterates” to provide convergence guarantees independent of delays. More recently, Even et al. (2024) proposed a unified framework for convergence analysis of distributed algorithms based on the AGRAP framework. There have been lots of other analysis methods proposed for deriving convergence guarantees for asynchronous distributed SGD (see Assran et al. (2020) for a survey). In our work, we propose an entirely novel framework that hasn’t been used before based on stochastic differential equations, and provide convergence guarantees of the algorithm to a stationary distribution centered around the local optima of conventional BP.

Communication-efficient algorithms. One of the bottlenecks when training on multiple devices or nodes in parallel is the synchronization step. The bigger or deeper the models get, the more time is consumed by synchronization. PowerSGD computes low-rank approximations of the gradients using power iteration methods. Poseidon (Zhang et al., 2017) also factorizes gradients matrices but interleaves their communication with the backward pass. Wen et al. (2017) and Alistarh et al. (2017) quantize gradients to make them lightweight for communication. Like Zhang et al. (2017), we interleave the backward pass with gradients communication but without gradients averaging.

Block local learning. Dividing the network across multiple devices and performing local updates is a widely recognized approach in distributed learning. The backward passes of the different blocks can be done simultaneously. The global loss is used to provide feedback only to the output block while the remaining blocks get learning signals from auxiliary networks which each compute local targets. Ma et al. (2024) uses a shallower version of the network as the auxiliary network at each layer. Gomez et al. (2022) allows gradients to flow to k-neighboring blocks. Nøkland & Eidnes (2019) don't allow gradients to flow to neighboring blocks, and instead use an auxiliary matching loss and a local cross-entropy loss to compute the local error. Decoupled Parallel Backpropagation (Huo et al., 2018) does full Backpropagation but uses stale gradients in the blocks to avoid update locking. Kappel et al. (2023) take a probabilistic approach by interpreting layers outputs as parameters of a probability distribution. Auxiliary networks provide local targets, which are used to train each block individually. Similar to these distributed paradigms, we mimic the execution of multiple backward passes in parallel by reordering the training sequence but without splitting the network explicitly during forward and backward propagation.

3 METHODS

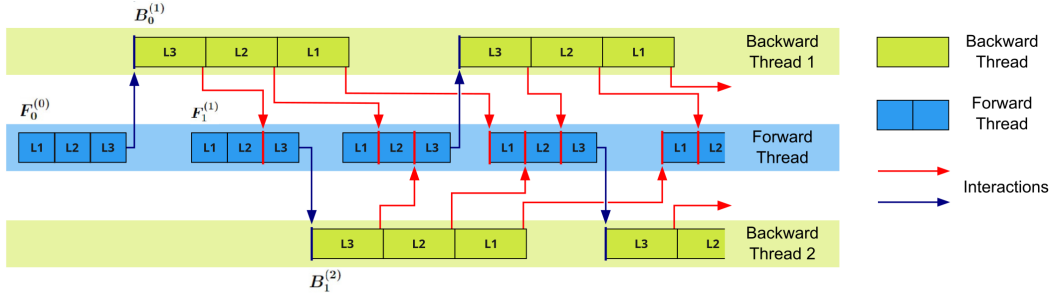


Figure 1: Illustration of decoupled backpropagation with separate threads for the forward and backward passes and the layer-wise updates. For each thread, the order of computations for a sample network with three layers denoted L1, L2 and L3, are shown. Arrows denote dependencies across threads. Within each thread, the computations for each layer are performed sequentially, whereas across threads, the dependencies are layer-wise. Interactions for 2 backward threads and a single forward thread are shown. This asynchronous interaction, along with layer-wise updates, reduces the staleness of parameters.

3.1 ASYNCHRONOUS FORMULATION OF BACKPROPAGATION

We introduce a new asynchronous stochastic gradient descent method where, instead of performing the forward and backward phases sequentially, we execute them in parallel and perform layer-wise parameter updates as soon as the gradients for a given layer are available. The dependencies between forward and backward phases are illustrated in Figure 1.

Since the gradient computation in the backward pass tends to consume more time than the loss calculation in the forward pass, we decouple these two into separate threads and use one forward thread and two backward threads to counterbalance the disproportionate execution time.

Figure 1 illustrates the interaction among threads based on one example. Initially, only the first forward pass, $F_0^{(0)}$, is performed. The resulting loss is then used in the first backward pass $B_0^{(1)}$,

which starts in parallel to the second forward pass $F_1^{(1)}$. Once $F_1^{(1)}$ ends, its loss is used by $B_1^{(2)}$ running in parallel to the next forward pass and $B_0^{(1)}$.

3.2 LAYER-WISE UPDATES

Parallelizing the forward and backward passes can speed up training, but it violates several key assumptions of Backpropagation leading to sub-optimal convergence observed in different studies (Keuper & Preundt, 2016; Zheng et al., 2017). This happens because the losses and gradients are often calculated using inconsistent and outdated parameters.

To alleviate this problem, we update the layers as soon as the corresponding gradients are available from the backward pass. $F_1^{(1)}$ receives partial parameter updates from $B_0^{(1)}$ as soon as they are available. Therefore, the parameters used in $F_1^{(1)}$ will differ from those used in $F_0^{(0)}$ because some layers of the model would have been already updated by the thread $B_0^{(1)}$. On average, we can expect that the second half of the layers use a new set of parameters. It is important to note that the updates happen without any locking mechanism and asynchronous to the backward pass as done by Zhang et al. (2017).

3.3 SPEED-UP ANALYSIS

Before discussing experimental results, we study the potential speed-up of the asynchronous with layer-wise updates formulation over standard Backpropagation. To arrive at this result, we make the following assumptions to estimate the performance gain

- We assume that there are no delays between the end of a forward pass, the beginning of its corresponding backward pass and the next forward pass. This implies for example that as soon as $F_0^{(0)}$ ends, $F_1^{(1)}$ and $B_0^{(1)}$ begin immediately. Multiples backward threads are therefore running in parallel.
- Vanilla Backpropagation performs b forward passes. We assume that this number also corresponds to the number of backward passes and the number of batches of data to be trained on.
- A forward pass lasts T units of time and a backward pass βT units of time, with a scaling factor $\beta > 1$ (expected to be at around 2 as show in appendix A.3).

The speed-up factor λ observed can be express as the fraction between the estimated time taken by the standard over the Async version of BP. Let T_1 be the time taken by BP to be trained on b batches of data. Because the forward and backward passes are sequential for each batch of data, we have:

$$\begin{aligned} T_1 &= Tb + b\beta T \\ &= (b + \beta)T . \end{aligned}$$

Now let T_2 be the time taken by the asynchronous algorithm to be trained on b batches of data, and n be the number of remaining backward passes to be executed after all the forward passes have been performed.

We have $n = \beta$ and $T_2 = bT + nT = Tb + \beta T$. The speed-up factor λ is the ratio of T_1 by T_2 , which by inserting the results above gives

$$\lambda = \frac{(1 + \beta)b}{(b + \beta)} .$$

By taking the limit of large number of batches, $b \rightarrow \infty$, we have

$$\lambda = 1 + \beta .$$

Hence, the maximum achievable speedup is expected to be $1 + \beta$, where β is the scaling factor of the backward pass time. In practice, the speed-up factor λ can be influenced by multiples factors like data loading which is sometimes a bottleneck (Leclerc et al., 2023; Isenko et al., 2022), or the system overhead, which reduce the achievable speedup.

3.4 STALENESS ANALYSIS

Here, we demonstrate the advantage of applying layer-wise updates (LU) compared to block updates (BU). BU refers to performing updates only after the entire backward pass is complete, a technique used in various previous asynchronous learning algorithms, e.g. (Recht et al., 2011; Chatterjee et al., 2022; Zheng et al., 2017). We use the same notation as in section 3.3.

To express this formally, we define the relative staleness τ of BU compared to LU as the time delay between when the gradients become available and when they are used to update the model weights. The intuition behind this lies in the fact that the more the updates are postponed, the more likely the gradients will become stale. The staleness will only increase with time and accumulate across the layers. Assuming that the time required to compute the gradients for each layer is uniform and equal to $\frac{\beta T}{M}$, the relative staleness is expressed as $\tau = \frac{\beta T(M-1)}{2}$.

To see this, we use that by definition, the staleness increases as we approach the output layer. At any layer m , the layer-wise staleness $\tau_m = \frac{\beta T}{M}m$. Averaging over the layers, we have

$$\tau = \sum_{m=1}^M \tau_m = \frac{\beta T}{M} \sum_{m=1}^M m = \beta T \frac{(M-1)}{2}$$

Clearly, τ increases with the network’s depth and the time required to perform one backward pass. Thus, the speedup is expected to scale approximately linearly with the network depth, showing the advantage of LU over BU for large M .

3.5 ALGORITHM

The Async BP algorithm is illustrated in Figure 1 and described in Algorithm listing 1. The algorithm consists of two components: a single forward thread and multiple backward threads. All threads work independently and asynchronously without any locking mechanism.

The forward thread is solely responsible for computing the loss $\mathcal{L}_i(\theta^u, \mathbf{x}_i, \mathbf{y}_i)$, given the current mini batch of data $(\mathbf{x}_i, \mathbf{y}_i) \in \mathcal{D}$ and the latest set of updated weights θ^u . Since the algorithm works asynchronously, the weights θ^u can be updated by any backward thread even while forward pass progresses. Once the forward pass is done, \mathcal{L}_i is sent to one of the backward threads and the forward thread moves to the next batch of data.

In parallel, a backward thread k receives a loss \mathcal{L}_j and performs the backward pass. At each layer m , the gradients $G(\theta_{m,k}^v) = \frac{\partial \mathcal{L}_j}{\partial \theta_{m,k}^v}$ are computed, after which $\theta_{m,k}^v$ is immediately used to update the forward thread parameters. Note that the backward thread here can potentially calculate the gradients for a different values of parameters $\theta_{m,k}^v$ than the ones used for the forward pass θ^u . In Section 5 and appendix B we show that this algorithm closely approximates conventional stochastic gradient descent, if asynchronous parameter updates arrive sufficiently frequent.

4 RESULTS

We evaluate our method on three vision tasks, CIFAR-10, CIFAR-100 and Imagenet, and on one sequence modeling task: IMDB sentiment analysis. We use Resnet18 and Resnet50 architectures for vision tasks and a LSTM network for sequence modelling. These networks are trained on a machine with 3 NVIDIA A100 80GB PCIe GPUs with two AMD EPYC CPUs sockets of 64 cores each. The experiment code is based on the C++ frontend of Torch (Paszke et al., 2019) - Libtorch.

The Performance of these tasks is compared to Locally-Asynchronous-Parallel SGD (LAPSGD) and Locally-Partitioned-Asynchronous-Parallel SGD (LPPSGD) (Chatterjee et al., 2022). These methods extend the well-known Hogwild! algorithm and Partitioned Asynchronous Stochastic Sub-gradient (PASSM+) to multiple devices, respectively.

We record the achieved accuracy on the tasks and the wall-clock time to reach a target accuracy (TTA). If not stated otherwise, this accuracy is chosen to be the best accuracy achieved by the worst performing algorithm. We used the code made available by Chatterjee et al. (2022) which uses Pytorch Distributed Data-Parallel API.

Algorithm 1 Async BP with decoupled partial updates

Forward thread

Given: Data: $(x_i, y_i) \in \mathcal{D}$, latest up-to-date parameters: θ^u
Compute $\mathcal{L}_i(\theta^u, x_i, y_i)$
send(\mathcal{L}_i) // send loss to a backward thread

Backward Thread k (running in parallel to the forward thread)

Given: Loss: \mathcal{L}_j , learning rate: η
for layer $m \in [M, 1]$ **do**
 Compute $G(\theta_{m,k}^v)$
 $\theta_{m,k}^{v+1} \leftarrow \theta_{m,k}^v - \eta \cdot G$
 $\theta_m \leftarrow \theta_{m,k}^{v+1}$ // asynchronously update forward thread
end for

4.1 ASYNCHNOUS TRAINING OF VISION TASKS

We follow the training protocol of LAPSGD and LPPSGD and chose the number of processes per GPU to be 1 since the GPU utilization was close to 100%. We trained them with a batch size of 128 per-rank. We used Stochastic gradient descent (SGD) for both Async BU and LU, with an initial learning rate of 0.005 for 5 epochs and 0.015 after the warm-up phase, a momentum of 0.9 and a weight decay of 5×10^{-2} . We use a cosine annealing schedule with a T_{max} of 110. We trained Resnet-50 on Imagenet-1K task (Table 5) for a total of 300 epochs with the same learning rate but with a cosine schedule with T_{max} of 250 and weight decay of 3.5×10^{-2} . Although, the simulations were run with cosine annealing scheduler, implying the ideal number of training epochs, early stopping was applied, i.e. training was stopped if no improvement of the accuracy was achieved for 30 epochs.

As shown below, Async LU achieves the highest accuracies while Async BU converges the fastest in terms of time to reach the target accuracy. The CIFAR-10 and CIFAR-100 results are presented in Tables 1, 2 and Tables 3, 4 respectively. In Tables 1 and 3, the time to target accuracy (TTA) is chosen to be the time taken to achieved the best accuracy reached by the worst algorithm. Whereas in Tables 2 and 4, it represents taken by an algorithm achieve its best accuracy. Async BU achieves a speed-up of up to $2.97 \times$ over LPPSGD on CIFAR100 (see Table 3). The poor performance of both LAPSGD and LPPSGD can be explained by the influence of staleness, thus requiring large number of training epochs.

We also achieved promising results on the ImageNet-1k dataset (see Table 5). Async LU achieved 73% accuracy $\times 3$ faster than Backpropagation on single GPU, showing potential of ideal linear scaling. An extensive comparison of Async LU with multi-GPU Backpropagation (Data Distributed Parallel) is provided in appendix A.2.

Although Async BU converges quicker than Async LU, it reaches lower accuracy. This is particularly visible on CIFAR100, a harder task than CIFAR10 (see Figures 2 and 3). Overall, Async BU showed a good balance between convergence speed and reduction of staleness.

4.2 ASYNCHRONOUS TRAINING OF SEQUENCE MODELLING TASK

For demonstrating Async BP training on sequence modelling, we evaluated an LSTM networks on the IMDb dataset (Maas et al., 2011). Sentiment analysis is the task of classifying the polarity of a given text. We used a 2-Layer LSTM network with 256 hidden dimensions to evaluate this task. We trained the network until convergence using the Adam optimizer with an initial learning rate of 1×10^{-2} . Results are shown in Table 6.

Table 1: Comparison of Async LU, Async BU, LAPSGD and LPPSGD based on time to reach accuracy (TTA): 87% for ResNet18 and 89% for ResNet50, and the number of epochs to reach the target for 3 runs on CIFAR10.

Network architecture	Training method	TTA (in seconds) mean \pm std	Epochs mean \pm std
ResNet-18	Async LU	223.8 \pm 28	65 \pm 10
	Async BU	173.4 \pm 2	64 \pm 2
	LAPSGD	706.3 \pm 13	104 \pm 2
	LPPSGD	461.0 \pm 7	86 \pm 1
ResNet-50	Async LU	737.9 \pm 24	86 \pm 6
	Async BU	700.6 \pm 20	86 \pm 1
	LAPSGD	999.5 \pm 38	117 \pm 3
	LPPSGD	863.4 \pm 35	119 \pm 1

Table 2: Comparison of Async LU, Async BU, LAPSGD, and LPPSGD based on best accuracy, time to reach accuracy (TTA), and epoch at the accuracy is achieved for 3 runs on CIFAR10.

Network architecture	Training method	Best accuracy mean \pm std	TTA (in seconds) mean \pm std	Epochs mean \pm std
ResNet-18	Async LU	93.7 \pm 0.28	380.7 \pm 33	114 \pm 9
	Async BU	92.7 \pm 0.16	308.5 \pm 14	115 \pm 2
	LAPSGD	88.2 \pm 0.43	799.5 \pm 20	118 \pm 2
	LPPSGD	87.8 \pm 0.09	523.4 \pm 15	97 \pm 1
ResNet-50	Async LU	93.9 \pm 0.10	1038.8 \pm 61	121 \pm 6
	Async BU	93.2 \pm 0.25	953.7 \pm 73	116 \pm 8
	LAPSGD	89.7 \pm 0.27	1098.9 \pm 30	117 \pm 3
	LPPSGD	89.3 \pm 0.43	888.4 \pm 37	119 \pm 1

We observe that although both Async LU and Async BU achieve the same accuracy, performing layer-wise updates reduces the training time and number of steps to convergence almost by half (see Figure 4 in Appendix A) highlighting again the importance of this strategy.

5 THEORETICAL ANALYSIS OF CONVERGENCE

Here, we theoretically analyse the convergence behavior of the algorithm outlined above. For the theoretical analysis, we consider the general case of multiple threads, acting on the parameter set θ , such that the threads interact asynchronously and can work on outdated versions of the parameters. We model the evolution of the learning algorithm as a continuous-time stochastic process (Bellec et al., 2017) to simplify the analysis. This assumption is justified by the fact that learning rates are typically small, and therefore the evolution of network parameters is nearly continuous.

In the model studied here, the stochastic interaction between threads is modelled as noise induced by random interference of network parameters. To arrive at this model, we use the fact that the dynamics of conventional stochastic gradient descent (SGD) can be modelled as the system of stochastic differential equations that determine the dynamics of the parameter vector θ

$$d\theta_k = -\eta \frac{\partial}{\partial \theta_k} \mathcal{L}(\theta) dt + \frac{\eta \sigma_{\text{SGD}}}{\sqrt{2}} dW_k, \quad (2)$$

with learning rate η and where dW_k are stochastic changes of the Wiener processes.

Eq. 2 describes the dynamics of a single parameter θ_k . The dynamics is determined by the gradient of the loss function \mathcal{L} , and the noise induced by using small mini-batches modelled here as idealized Wiener process with amplitude σ_{SGD} . Because of this noise, SGD does not strictly converge to a local optimum but maintains a stationary distribution $p^*(\theta_k) \propto e^{-\frac{1}{\eta} \mathcal{L}(\theta_k)}$, that assigns most of the probability mass to parameter vectors that reside close to local optima (Bellec et al., 2017).

Table 3: Comparison of Async LU, Async BU, LAPSGD and LPPSGD based on time to reach accuracy (TTA): 60% for ResNet18 and 63% for ResNet50, and the number of epochs to reach the target for 3 runs on CIFAR100.

Network architecture	Training method	TTA (in seconds) mean \pm std	Epochs mean \pm std
ResNet-18	Async LU	226.4 \pm 10	69 \pm 7
	Async BU	155.4 \pm 10	57 \pm 4
	LAPSGD	667.1 \pm 8	99 \pm 2
	LPPSGD	672.9 \pm 11	100 \pm 2
ResNet-50	Async LU	622.7 \pm 32	70 \pm 5
	Async BU	641.8 \pm 16	81 \pm 3
	LAPSGD	1006.6 \pm 13	107 \pm 1
	LPPSGD	1016.0 \pm 6	107 \pm 1

Table 4: Comparison of Async LU, Async BU, LAPSGD and LPPSGD based on best accuracy, time to reach accuracy (TTA), and epoch at the accuracy is achieved for 3 runs on CIFAR100.

Network architecture	Training method	Best accuracy mean \pm std	TTA (in seconds) mean \pm std	Epochs mean \pm std
ResNet-18	Async LU	73.9 \pm 0.38	339.0 \pm 10	114 \pm 9
	Async BU	71.8 \pm 0.08	277.2 \pm 17	103 \pm 5
	LAPSGD	61.3 \pm 0.23	762.5 \pm 15	114 \pm 3
	LPPSGD	61.0 \pm 0.17	742.0 \pm 19	110 \pm 2
ResNet-50	Async LU	76.2 \pm 0.57	1071.0 \pm 80	122 \pm 6
	Async BU	73.7 \pm 0.23	956.2 \pm 28	123 \pm 4
	LAPSGD	63.7 \pm 0.33	1110.1 \pm 27	118 \pm 3
	LPPSGD	63.5 \pm 0.10	1122.1 \pm 24	119 \pm 2

In the concurrent variant of SGD studied here, however, the dynamics is determined by perturbed gradients for different stale parameters. When updating the network using the described asynchronous approach without locking, we potentially introduce noise in the form of partially stale parameters or from one thread overwriting the updates of another. This noise will introduce a deviation from the ideal parameter vector θ . We model this deviation as additive Gaussian noise $\xi \sim \mathcal{N}(0, \sigma_{\text{STALE}})$ to the current parameter vector with variance σ_{STALE} . To approximate the noisy loss function, we use a first-order Taylor expansion around the noise-free parameters:

$$\begin{aligned} \mathcal{L}(\theta + \xi) &= \mathcal{L}(\theta) + \nabla_{\theta} \mathcal{L}(\theta)^{\top} \xi + \mathcal{O}(\sigma^2) \\ &\approx \mathcal{L}(\theta) + \nabla_{\theta} \mathcal{L}(\theta)^{\top} \xi, \end{aligned} \quad (3)$$

and thus the gradient can be approximated as

$$\nabla_{\theta} \mathcal{L}(\theta + \xi, \mathbf{X}, \mathbf{Y}) \approx \nabla_{\theta} \mathcal{L}(\theta) + \nabla_{\theta}^2 \mathcal{L}(\theta)^{\top} \xi. \quad (4)$$

Based on this, we can express the update rule as a Stochastic Differential Equation (SDE) and model the various noise terms using a Wiener Process \mathcal{W} . The noise sources in the learning dynamics come from two main sources, (1) noise caused by stochastic gradient descent, and (2) noise caused by learning with outdated parameters. We model the former as additive noise with amplitude σ_{STALE} and the latter using the Taylor approximation Eq. (4). Using this, we can write the approximate dynamics of the parameter vector θ as the stochastic differential equation

$$d\theta_k = \mu_k(\theta, t) + \sqrt{D_k(\theta)} d\mathcal{W}_k, \quad (5)$$

with

$$\begin{aligned} \mu_k(\theta) &= -\eta \frac{\partial}{\partial \theta_k} \mathcal{L}(\theta) \\ D_k(\theta) &= \frac{\eta^2 \sigma_{\text{SGD}}^2}{2} + \frac{\eta^2 \sigma_{\text{STALE}}^2}{2} \sum_l \frac{\partial^2}{\partial \theta_k \partial \theta_l} \mathcal{L}(\theta), \end{aligned} \quad (6)$$

Table 5: Classification accuracy (% correct) for Async LU (3 GPUs) and vanilla backpropagation (single GPU) on the ImageNet task.

Network architecture	training method	test-accuracy	train-accuracy	TTA (in 1000 seconds)
ResNet-50	Async LU	73.42	93.08	134.24
	BP (single GPU)	73.40	91.90	403.77

Table 6: Comparison of Async LU, Async BU based on best accuracy, time to reach accuracy (TTA), and epoch at the accuracy is achieved for 3 runs on IMDB

Network architecture		best accuracy mean \pm std	TTA(in seconds) mean \pm std	epoch mean \pm std
LSTM	Async LU	85.15 \pm 0.15	49.3 \pm 9.46	6 \pm 1
	Async BU	85.06 \pm 0.59	83.41 \pm 12.56	12 \pm 2

where μ_k is the drift and D_k the diffusion of the SDE.

In Appendix B we study the stationary distribution of this parameter dynamics. We show that the stationary distribution is a close approximation to p^* of SGD, which is perfectly recovered if σ_{STALE} is small compared to σ_{SGD} , i.e. if the effect of staleness is small compared to the noise induced by minibatch sampling.

6 DISCUSSION

In this work, we introduced a novel asynchronous approach to train deep neural networks that decouples the forward and backward passes and performs layer-wise parameter updates. Our method addresses key limitations of standard backpropagation by allowing parallel execution of forward and backward passes and mitigating update locking through asynchronous layer-wise updates.

The experimental results demonstrate that our approach can achieve comparable or better accuracy than synchronous backpropagation and other asynchronous methods across multiple vision and language tasks, while providing significant speedups in training time. On CIFAR-10 and CIFAR-100, we observed speedups of up to $2.97\times$ compared to asynchronous SGD covering a broad range of paradigms. The method also showed promising results on a sentiment analysis task and the ImageNet classification task where it reached close to ideal scaling.

Our theoretical analysis, based on modeling the learning dynamics as a continuous-time stochastic process, provides convergence guarantees and shows that the algorithm converges to a stationary distribution closely approximating that of standard SGD under certain conditions. This offers a solid foundation for understanding the behavior of our asynchronous approach.

While our implementation using C++ and LibTorch demonstrated the potential of this method, we also identified some limitations related to GPU resource allocation in SIMT architectures. Future work could explore optimizing the implementation for more efficient GPU utilization, or investigating hybrid CPU-GPU approaches to fully leverage the benefits of asynchronous execution.

Overall, this work presents a promising direction for scaling up deep learning through asynchronous, decoupled updates. The approach has the potential to enable more efficient training of large-scale models, particularly in distributed and heterogeneous computing environments. Further research could explore extensions to even larger models, additional tasks, and more diverse hardware setups to fully realize the potential of this asynchronous training paradigm.

REPRODUCIBILITY

We ensure that the results presented in this paper are easily reproducible using just the information provided in the main text as well as the supplement. Details of the models used in our simulations are presented in the main paper and further elaborated in the supplement. We provide additional details and statistics over multiple runs in the supplement section A.4. We use publicly available

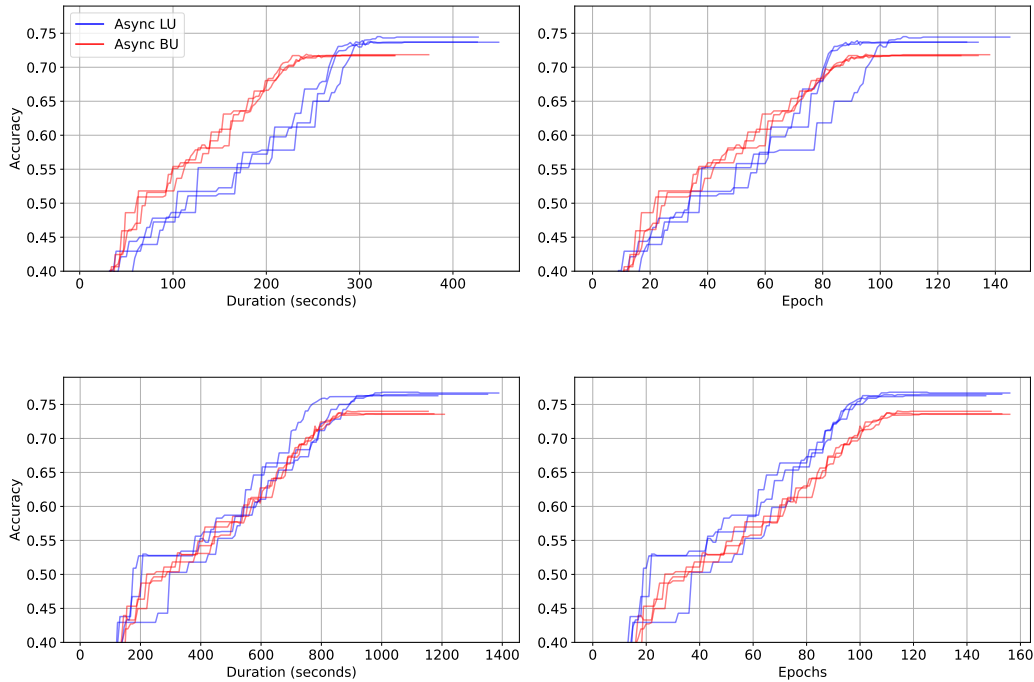


Figure 2: Learning curves of Asynchronous SGD with layer-wise updates (Async LU) and Block updates (Async BU) on the CIFAR100 dataset. 3 independent runs shown for each class.

libraries and datasets in our simulations. We will further provide the source code to the reviewers and ACs in an anonymous repository once the discussion forums are opened. This included code will also contain “readme” texts to facilitate easy reproducibility. The theoretical analysis provided in section 5 is derived in the supplement.

ACKNOWLEDGEMENTS

Cabrel Teguemne Fokam and Khaleelulla Khan Nazeer are funded by the German Federal Ministry of Education and Research (BMBF), funding reference 16ME0729K, joint project “EVENTS”. Lukas König and David Kappel are funded by the German Federal Ministry for Economic Affairs and Climate Action (BMWK) project ESCADE (01MN23004A). The authors gratefully acknowledge the Gauss Centre for Supercomputing e.V. (www.gauss-centre.eu) for funding this project by providing computing time on the GCS Supercomputer JUWELS at Jülich Supercomputing Centre (JSC).

REFERENCES

- Dan Alistarh, Demjan Grubic, Jerry Li, Ryota Tomioka, and Milan Vojnovic. Qsgd: Communication-efficient sgd via gradient quantization and encoding, 2017. URL <https://arxiv.org/abs/1610.02132>.
- Mahmoud Assran, Arda Aytekin, Hamid Reza Feyzmahdavian, Mikael Johansson, and Michael G Rabbat. Advances in asynchronous parallel and distributed optimization. *Proceedings of the IEEE*, 108(11):2013–2031, 2020.
- Gerard M Baudet. Asynchronous iterative methods for multiprocessors. *Journal of the ACM (JACM)*, 25(2):226–244, 1978.
- Guillaume Bellec, David Kappel, Wolfgang Maass, and Robert Legenstein. Deep rewiring: Training very sparse deep networks. *arXiv preprint arXiv:1711.05136*, 2017.

-
- Dimitri Bertsekas and John Tsitsiklis. *Parallel and distributed computation: numerical methods*. Athena Scientific, 2015.
- Bapi Chatterjee, Vyacheslav Kungurtsev, and Dan Alistarh. Scaling the wild: Decentralizing hogwild!-style shared-memory sgd, 2022. URL <https://arxiv.org/abs/2203.06638>.
- Mathieu Even, Anastasia Koloskova, and Laurent Massoulié. Asynchronous SGD on Graphs: A Unified Framework for Asynchronous Decentralized and Federated Optimization. In *Proceedings of The 27th International Conference on Artificial Intelligence and Statistics*, pp. 64–72. PMLR, April 2024. URL <https://proceedings.mlr.press/v238/even24a.html>.
- Aidan N. Gomez, Oscar Key, Kuba Perlin, Stephen Gou, Nick Frosst, Jeff Dean, and Yarin Gal. Interlocking backpropagation: improving depthwise model-parallelism. *J. Mach. Learn. Res.*, 23 (1), jan 2022. ISSN 1532-4435.
- Zhouyuan Huo, Bin Gu, qian Yang, and Heng Huang. Decoupled parallel backpropagation with convergence guarantee. In Jennifer Dy and Andreas Krause (eds.), *Proceedings of the 35th International Conference on Machine Learning*, volume 80 of *Proceedings of Machine Learning Research*, pp. 2098–2106. PMLR, 10–15 Jul 2018. URL <https://proceedings.mlr.press/v80/huo18a.html>.
- Alexander Isenko, Ruben Mayer, Jeffrey Jedicke, and Hans-Arno Jacobsen. Where is my training bottleneck? hidden trade-offs in deep learning preprocessing pipelines. In *Proceedings of the 2022 International Conference on Management of Data*, pp. 1825–1839, 2022.
- David Kappel, Khaleelulla Khan Nazeer, Cabrel Teguemne Fokam, Christian Mayr, and Anand Subramoney. Block-local learning with probabilistic latent representations, 2023.
- Janis Keuper and Franz-Josef Preundt. Distributed training of deep neural networks: Theoretical and practical limits of parallel scalability. In *2016 2nd workshop on machine learning in HPC environments (MLHPC)*, pp. 19–26. IEEE, 2016.
- Adarsh Kumar, Kausik Subramanian, Shivaram Venkataraman, and Aditya Akella. Doing more by doing less: how structured partial backpropagation improves deep learning clusters. In *Proceedings of the 2nd ACM International Workshop on Distributed Machine Learning*, pp. 15–21, 2021.
- Vyacheslav Kungurtsev, Malcolm Egan, Bapi Chatterjee, and Dan Alistarh. Asynchronous optimization methods for efficient training of deep neural networks with guarantees. *Proceedings of the AAAI Conference on Artificial Intelligence*, 35(9):8209–8216, May 2021. doi: 10.1609/aaai.v35i9.16999. URL <https://ojs.aaai.org/index.php/AAAI/article/view/16999>.
- Guillaume Leclerc, Andrew Ilyas, Logan Engstrom, Sung Min Park, Hadi Salman, and Aleksander Madry. Ffcv: Accelerating training by removing data bottlenecks. In *Proceedings of the IEEE/CVF Conference on Computer Vision and Pattern Recognition*, pp. 12011–12020, 2023.
- Chenxiang Ma, Jibin Wu, Chenyang Si, and Kay Chen Tan. Scaling supervised local learning with augmented auxiliary networks. *arXiv preprint arXiv:2402.17318*, 2024.
- Andrew L. Maas, Raymond E. Daly, Peter T. Pham, Dan Huang, Andrew Y. Ng, and Christopher Potts. Learning word vectors for sentiment analysis. In Dekang Lin, Yuji Matsumoto, and Rada Mihalcea (eds.), *Proceedings of the 49th Annual Meeting of the Association for Computational Linguistics: Human Language Technologies*, pp. 142–150, Portland, Oregon, USA, June 2011. Association for Computational Linguistics. URL <https://aclanthology.org/P11-1015>.
- Konstantin Mishchenko, Francis Bach, Mathieu Even, and Blake Woodworth. Asynchronous SGD Beats Minibatch SGD Under Arbitrary Delays, June 2022. URL <http://arxiv.org/abs/2206.07638>.

-
- Giorgi Nadiradze, Iliia Markov, Bapi Chatterjee, Vyacheslav Kungurtsev, and Dan Alistarh. Elastic Consistency: A Practical Consistency Model for Distributed Stochastic Gradient Descent. *Proceedings of the AAAI Conference on Artificial Intelligence*, 35(10):9037–9045, May 2021. ISSN 2374-3468. doi: 10.1609/aaai.v35i10.17092. URL <https://ojs.aaai.org/index.php/AAAI/article/view/17092>.
- Arild Nøkland and Lars Hiller Eidnes. Training neural networks with local error signals. In *International conference on machine learning*, pp. 4839–4850. PMLR, 2019.
- Adam Paszke, Sam Gross, Francisco Massa, Adam Lerer, James Bradbury, Gregory Chanan, Trevor Killeen, Zeming Lin, Natalia Gimelshein, Luca Antiga, Alban Desmaison, Andreas Kopf, Edward Yang, Zachary DeVito, Martin Raison, Alykhan Tejani, Sasank Chilamkurthy, Benoit Steiner, Lu Fang, Junjie Bai, and Soumith Chintala. Pytorch: An imperative style, high-performance deep learning library. In *Advances in Neural Information Processing Systems 32*, pp. 8024–8035. Curran Associates, Inc., 2019. URL https://proceedings.neurips.cc/paper_files/paper/2019/file/bdbca288fee7f92f2bfa9f7012727740-Paper.pdf.
- Benjamin Recht, Christopher Re, Stephen Wright, and Feng Niu. Hogwild!: A lock-free approach to parallelizing stochastic gradient descent. In J. Shawe-Taylor, R. Zemel, P. Bartlett, F. Pereira, and K.Q. Weinberger (eds.), *Advances in Neural Information Processing Systems*, volume 24. Curran Associates, Inc., 2011. URL https://proceedings.neurips.cc/paper_files/paper/2011/file/218a0aefd1d1a4be65601cc6ddc1520e-Paper.pdf.
- Wei Wen, Cong Xu, Feng Yan, Chunpeng Wu, Yandan Wang, Yiran Chen, and Hai Li. Terngrad: Ternary gradients to reduce communication in distributed deep learning, 2017. URL <https://arxiv.org/abs/1705.07878>.
- Paul Werbos. Applications of advances in nonlinear sensitivity analysis. *System Modeling and Optimization*, pp. 762–770, 1982.
- Hao Zhang, Zeyu Zheng, Shizhen Xu, Wei Dai, Qirong Ho, Xiaodan Liang, Zhiting Hu, Jintao Wei, Pengtao Xie, and Eric P. Xing. Poseidon: An efficient communication architecture for distributed deep learning on GPU clusters. In *2017 USENIX Annual Technical Conference (USENIX ATC 17)*, pp. 181–193, Santa Clara, CA, July 2017. USENIX Association. ISBN 978-1-931971-38-6. URL <https://www.usenix.org/conference/atc17/technical-sessions/presentation/zhang>.
- Shuxin Zheng, Qi Meng, Taifeng Wang, Wei Chen, Nenghai Yu, Zhi-Ming Ma, and Tie-Yan Liu. Asynchronous stochastic gradient descent with delay compensation. In *International conference on machine learning*, pp. 4120–4129. PMLR, 2017.

A FURTHER RESULTS

A.1 LEARNING CURVES

Here, we provide additional details to the CIFAR10 and IMDB results provided in the main text. Figures 3 and 4 show the learning dynamics of Asynchronous Backpropagation with blocks updates (Async BU) and with layer-wise updates (Async LU) on CIFAR10 and IMDB respectively. The difference in convergence speed and accuracy observed with CIFAR100 2 is less noticeable on CIFAR10, probably because it is a simpler task. However, we clearly see the advantage of Async LU on the IMDB, where it not only converges faster but also to similar accuracy.

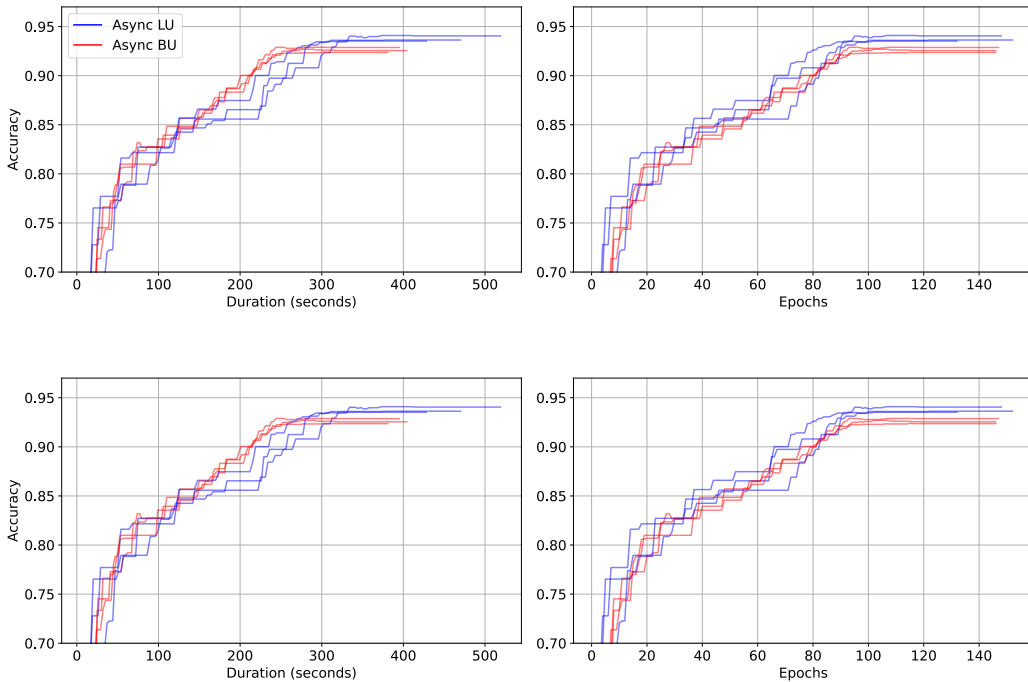


Figure 3: Learning curves of Asynchronous SGD with layer-wise updates (Async LU) and Block updates (Async BU) for ResNet18 (top plots) and ResNet50 (bottom plots) on the CIFAR10 dataset.

A.2 SPEED-UP COMPARISON WITH MULTI-GPU BACKPROPAGATION

Here we do a comparison of Asynchronous Backpropagation with layer-wise updates (Async LU) and multi-GPU Data Distributed Parallel(DDP) both trained on 3 GPUs residing on the same machine (described in section 4) to achieve their accuracies. Since Async LU uses only one forward pass, we set its batch size to be 128 and that of BP to $3\times$ higher (384). Async LU was implemented on the c++ library of Pytorch, Libtorch, and implemented using Pytorch DataDistributedParallel (DDP) API. The hyperparameters used are the same as described in section 4.

To make the comparison fair, the relative speed-up is calculated with respect of the single GPU implementation of Backpropagation on Libtorch for Async LU and Pytorch for DDP.

In this Settings, DDP should clearly the advantages since it uses a bigger batch size and all the GPUs are on the same machine, reducing considerably the communication bottleneck, hence making the synchronization step faster. However with observe that Async LU achieves comparable relative speed-up over single GPU compared to DDP on both CIFAR10 and CIFAR100. This shows the effectiveness of our asynchronous formulation (figure 1). We can expect Async LU to have some advantage in a multi-node or heterogeneous setting because the synchronization barrier becomes problem.

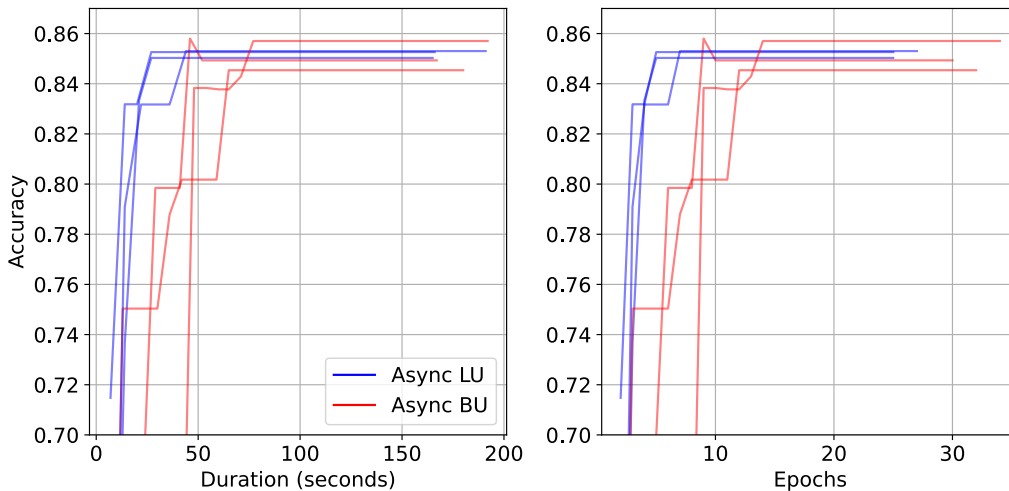


Figure 4: Learning curves of Asynchronous SGD with layer-wise updates (Async LU) and Block updates (Async BU) on the IMDb dataset.

Table 7: Comparison of Async LU and DDP both trained on 3GPUs based on their relative speed-up to single GPU implementation for 3 runs on CIFAR10

Network architecture	Training method	Relative speed-up mean \pm std
ResNet-18	Async LU	1.86 ± 0.21
	DDP	1.90 ± 0.08
ResNet-50	Async LU	2.02 ± 0.10
	DDP	2.38 ± 0.19

A.3 TIME MEASUREMENTS

Here we provide the results of a small scale experiment on the timing measurement of forward and backward passes for CIFAR-100 with batch size 128 in table 9. As expected, a single backward requires $2\times$ of a single backward pass. Extensive experiments on this is provided by Kumar et al. (2021)

A.4 HYPERPARAMETERS FOR THE EXPERIMENTS

Hyperparameters used in training experiments presented in section 4 are documented in table 10

B CONVERGENCE PROOF

Here we provide the proof that the stochastic parameter dynamics, Eq. (5) of the main text, converges to a stationary distribution $p^*(\theta)$ given by

$$p^*(\theta) = \frac{1}{Z} \exp\left(\sum_k h_k(\theta)\right), \text{ with } h_k(\theta) = \int \frac{\mu_k(\theta)}{D_k(\theta)} d\theta - \ln |D_k(\theta)| + C. \quad (7)$$

The proof is analogous to the derivation given in Bellec et al. (2017), and relies on stochastic calculus to determine the parameter dynamics in the infinite time limit. Since the dynamics include a noise term, the exact value of the parameters $\theta(t)$ at a particular point in time $t > 0$ cannot be determined, but we can describe the distribution of parameters using the Fokker-Planck formalism, i.e. we describe the parameter distribution at time t by a time-varying function $p_{\text{FP}}(\theta, t)$.

Table 8: Comparison of Async LU and DDP both trained on 3GPUs based on their relative speed-up to single GPU implementation for 3 runs on CIFAR100

Network architecture	Training method	Relative speed-up mean \pm std
ResNet-18	Async LU	1.83 \pm 0.06
	DDP	1.86 \pm 0.21
ResNet-50	Async LU	2.02 \pm 0.13
	DDP	2.30 \pm 0.13

Table 9: Timing measurement of forward and backward passes for CIFAR-100 with batch size 128. Averaged over all batches for 15 epochs.

Network architecture	Forward pass (s) mean \pm std	Backward pass (s) mean \pm std
ResNet-18	0.0049 \pm 1E-04	0.0102 \pm 1E-04
ResNet-50	0.0166 \pm 5E-05	0.0299 \pm 4E-05

To arrive at an analytical solution for the stationary distribution, $p^*(\boldsymbol{\theta})$ we make the adiabatic assumption that noise in the parameters only has local effects, such that the diffusion due to noise in any parameter θ_j has negligible influence on dynamics in θ_k , i.e. $\frac{\partial}{\partial \theta_j} D_k(\boldsymbol{\theta}) = 0, \forall j \neq k$. Using this assumption, it can be shown that, for the dynamics (6), $p_{\text{FP}}(\boldsymbol{\theta}, t)$ converges to a unique stationary distribution in the limit of large t and small noise σ_{STALE} . To prove the convergence to the stationary distribution, we show that it is kept invariant by the set of SDEs Eq. (6) and that it can be reached from any initial condition. Eq. 6 implies a Fokker-Planck equation given by

$$\frac{\partial}{\partial t} p_{\text{FP}}(\boldsymbol{\theta}, t) = - \sum_k \frac{\partial}{\partial \theta_k} [\mu_k(\boldsymbol{\theta}, t) p_{\text{FP}}(\boldsymbol{\theta}, t)] + \frac{\partial^2}{\partial \theta_k^2} [D_k(\boldsymbol{\theta}, t) p_{\text{FP}}(\boldsymbol{\theta}, t)] \quad (8)$$

We show that, under the assumptions outlined above, the stochastic parameter dynamics Eq. (6) of the main text, converges to the stationary distribution $p^*(\boldsymbol{\theta})$ (Eq. (7)).

Table 10

	CIFAR-100		CIFAR-10		Imagenet	IMDb
hyperparameter	Resnet-18	Resnet-50	Resnet-18	Resnet-50	Resnet-50	LSTM
batch_size	128	128	128	128	300	75
lr	0.015	0.015	0.015	0.015	0.015	0.001
momentum	0.9	0.9	0.9	0.9	0.9	0.9
T_max	100	120	105	120	250	150
warm_up_epochs	5	5	3	5	5	0
warm_up_lr	0.005	0.005	0.005	0.005	0.0035	-
weight_decay	0.005	0.005	0.005	0.005	0.0035	0

To arrive at this result, we plug in the assumed stationary distribution into Eq. (8) and show the equilibrium $\frac{\partial}{\partial t} p_{\text{FP}}(\boldsymbol{\theta}, t) = 0$, i.e.

$$\begin{aligned}
\frac{\partial}{\partial t} p_{\text{FP}}(\boldsymbol{\theta}, t) &= - \sum_k \frac{\partial}{\partial \theta_k} [\mu_k(\boldsymbol{\theta}) p_{\text{FP}}(\boldsymbol{\theta}, t)] \\
&\quad + \frac{\partial^2}{\partial \theta_k^2} [D_k(\boldsymbol{\theta}) p_{\text{FP}}(\boldsymbol{\theta}, t)] = 0 \\
\leftrightarrow & - \sum_k \frac{\partial}{\partial \theta_k} [\mu_k(\boldsymbol{\theta}) p_{\text{FP}}(\boldsymbol{\theta}, t)] \\
&\quad + \frac{\partial}{\partial \theta_k} \left[\left(\frac{\partial}{\partial \theta_k} D_k(\boldsymbol{\theta}) \right) p_{\text{FP}}(\boldsymbol{\theta}, t) \right] \\
&\quad + \frac{\partial}{\partial \theta_k} \left[D_k(\boldsymbol{\theta}) \left(\frac{\partial}{\partial \theta_k} h_k(\boldsymbol{\theta}) \right) p_{\text{FP}}(\boldsymbol{\theta}, t) \right], \tag{9}
\end{aligned}$$

where we used the simplifying assumption, $\frac{\partial}{\partial \theta_j} D_k(\boldsymbol{\theta}) = 0, \forall j \neq k$, as outlined above. Next, using $\frac{\partial}{\partial \theta_j} h_k(\boldsymbol{\theta}) = \frac{1}{D_k(\boldsymbol{\theta}, t)} \left(\mu_k(\boldsymbol{\theta}, t) - \frac{\partial}{\partial \theta_j} D_k(\boldsymbol{\theta}, t) \right)$, we get

$$\begin{aligned}
\frac{\partial}{\partial t} p_{\text{FP}}(\boldsymbol{\theta}, t) = 0 \quad \leftrightarrow & - \sum_k \frac{\partial}{\partial \theta_k} [\mu_k(\boldsymbol{\theta}, t) p_{\text{FP}}(\boldsymbol{\theta}, t)] \\
& + \frac{\partial}{\partial \theta_k} \left[\left(\frac{\partial}{\partial \theta_k} D_k(\boldsymbol{\theta}, t) \right) p_{\text{FP}}(\boldsymbol{\theta}, t) \right] \\
& + \frac{\partial}{\partial \theta_k} \left[\left(\mu_k(\boldsymbol{\theta}, t) - \frac{\partial}{\partial \theta_k} D_k(\boldsymbol{\theta}, t) \right) p_{\text{FP}}(\boldsymbol{\theta}, t) \right] = 0 \tag{10}
\end{aligned}$$

This shows that the simplified dynamics, Eq. 6, leave the stationary distribution (7) unchanged.

This stationary distribution $p^*(\boldsymbol{\theta})$ is a close approximation to SGD. To see this, we study the maxima of the distribution, by taking the derivative

$$\frac{\partial}{\partial \theta_k} h_k(\boldsymbol{\theta}) = \frac{\mu_k(\boldsymbol{\theta})}{D_k(\boldsymbol{\theta})} - \frac{\partial}{\partial \theta_k} \ln |D_k(\boldsymbol{\theta})|, \tag{11}$$

which by inserting (6) can be written as

$$\frac{\partial}{\partial \theta_k} h_k(\boldsymbol{\theta}) = - \frac{1}{\eta} \frac{\nabla_{\theta} \mathcal{L}(\boldsymbol{\theta}) + \sigma_{\text{STALE}}^2 \nabla_{\theta}^3 \mathcal{L}(\boldsymbol{\theta})}{\sigma_{\text{SGD}}^2 + \sigma_{\text{STALE}}^2 \nabla_{\theta}^2 \mathcal{L}(\boldsymbol{\theta})} \tag{12}$$

If σ_{STALE} is small compared to σ_{SGD} we recover the canonical results for SGD $\frac{\partial}{\partial \theta_k} h_k(\boldsymbol{\theta}) \approx - \frac{1}{\eta} \frac{\nabla_{\theta} \mathcal{L}(\boldsymbol{\theta})}{\sigma_{\text{SGD}}^2}$, where smaller learning rates η make the probability of reaching local optima more peaked. Distortion of local optima, which manifests in the second term in the nominator, only depend on third derivatives, which can be expected to be small for most neural network architectures with well-behaved non-linearities.